

Footstep Parameterized Motion Blending using Barycentric Coordinates

Alejandro Beacco¹, Nuria Pelechano¹, Mubbasir Kapadia^{2,3} & Norman I. Badler³

¹Universitat Politècnica de Catalunya

²Rutgers University

³University of Pennsylvania

Abstract

This paper presents a real-time animation system for fully-embodied virtual humans that satisfies accurate foot placement constraints for different human walking and running styles. Our method offers a fine balance between motion fidelity and character control, and can efficiently animate over sixty agents in real time (25 FPS) and over a hundred characters at 13 FPS. Given a point cloud of reachable support foot configurations extracted from the set of available animation clips, we compute the Delaunay triangulation. At runtime, the triangulation is queried to obtain the simplex containing the next footstep, which is used to compute the barycentric blending weights of the animation clips. Our method synthesizes animations to accurately follow footsteps, and a simple IK solver adjusts small offsets, foot orientation, and handles uneven terrain. To incorporate root velocity fidelity, the method is further extended to include the parametric space of root movement and combine it with footstep based interpolation. The presented method is evaluated on a variety of test cases and error measurements are calculated to offer a quantitative analysis of the results achieved.

Keywords:

Character animation, Crowd simulation, Footsteps controller

1. Introduction

Crowd simulation research has matured in recent years with important applications in training, building design, psychological studies, and video-games. All these applications benefit from having fully-embodied virtual human characters animated in real-time while accurately satisfying control objectives without any noticeable artifacts.

Algorithms that generate center of mass (COM) trajectories [1, 2, 3, 4] lead to ambiguities when trying to superimpose a fully articulated virtual human to follow them, thus producing foot-sliding artifacts when no suitable animation is found, or when the root orientation and the displacement vector of the animation do not match. Different animations can be blended by tweaking some of the upper body joints [5] to minimize artifacts, at the expense of constant updates to account for the decoupling between the crowd simulation and the animation system.

Footstep-based control systems [6, 7] output a list of space-time foot-plants to define a fine-grained trajectory with fewer ambiguities that can solve more complex scenarios (e.g., complex manipulation tasks requiring careful control of the lower body, or collaborative tasks, such as careful sidestepping to make way for another agent in a narrow corridor). To realistically represent such simulations, we need a method to synthesize animations that accurately follow the output trajectory, i.e., accurate placement of feet with space-time constraints. This problem is traditionally known as the *stepping stone* problem.

Moreover, the output trajectory can be modified by external perturbations such as uneven terrain.

We present an online animation synthesis technique for fully embodied virtual humans that satisfies foot placement constraints for a large variety of locomotion speeds and styles (see Fig. 1). Given a database of motion clips, we precompute multiple parametric spaces based on the motion of the root and the feet. A root parametric space is used to compute a weight for each available animation based on root velocity. Two foot parametric spaces are based on a Delaunay triangulation of the graph of possible foot landing positions. For each foot parametric space, blending weights are calculated as the barycentric coordinates of the next footstep position for the triangle in the graph that contains it. These weights are used for synthesizing animations that accurately follow the footstep trajectory while respecting the singularities of the different walking styles captured.

Blending weights calculated as barycentric coordinates are used to reach the desired foot landing by interpolating between several proximal animations, and IK is used to adjust the final position of the support foot to correct for minor offsets, foot step orientation and the angle of the underlying floor.

Since foot parametric space only considers final landing positions of the feet without taking into account root velocity, this may lead to the selection of animations that satisfy position constraints but introduce discontinuities in root velocity. To incorporate root velocity fidelity we present a method that can integrate both foot positioning and root velocity fidelity. Our method also allows the system to recover nicely when the input

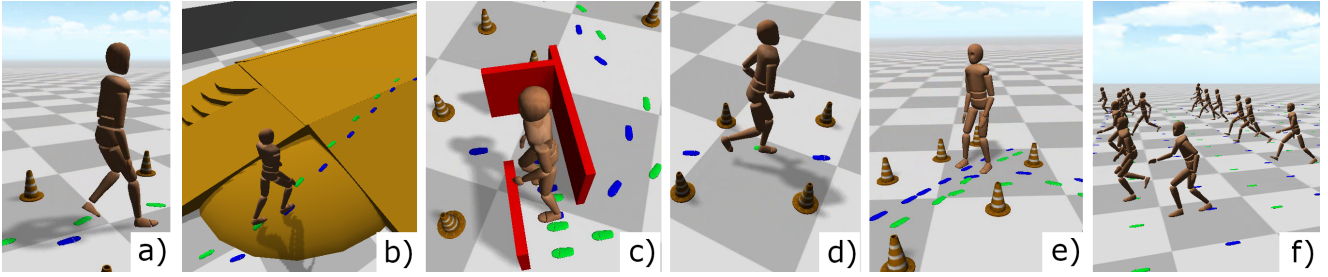


Figure 1: An autonomous virtual human navigating a challenging obstacle course (a), walking over a slope (b), exercising careful foot placement constraints including side-stepping (c), speed variations (d), and stepping back (e). The system can handle multiple agents in real time (f).

56 foot trajectory contains steps that are not possible to perform
 57 with the given set on animations (for example, due to extreme
 58 distance between steps).

59 The presented method is evaluated on a variety of test cases
 60 and error measurements are calculated to offer a quantitative
 61 analysis of the results achieved. Our framework can efficiently
 62 animate over sixty agents in real time (25 FPS) and over a hun-
 63 dred characters at 13 FPS, without compromising motion fi-
 64 delity or character control, and can be easily integrated into ex-
 65 isting crowd simulation packages. We also provide the user
 66 with control over the trade-off between footstep accuracy and
 67 root velocity.

68 2. Related Work

69 Locomotion synthesis can be tackled from different points
 70 of view depending on how the character is being controlled.
 71 If a user controls the character with a 3rd person controller, it
 72 is common to work on a root velocity basis, because the user
 73 wants to move the character around in an agile way. In such
 74 cases, like video-games, real-time response is critical and arti-
 75 facts such as foot skating can be ignored. Optimization based
 76 approaches [8] are able to synthesize animations that conform
 77 to velocity and orientation constraints. However, they need a
 78 very large database and their computational time does not al-
 79 low many characters in real-time. Semi-procedural animation
 80 systems [9] work with a small set of animations and use inverse
 81 kinematics only over the legs to ensure ground contact and to
 82 adapt the feet to possible slopes of the terrain, but they are un-
 83 able to follow footstep trajectories.

84 Animation systems for autonomous agents must be com-
 85 putationally efficient to animate a multitude of characters in
 86 real-time, and need to follow different control trajectories, de-
 87 pending on the controller used. Controllers that account for an-
 88 imation constraints while computing control decisions such as
 89 motion graphs [10, 11, 12, 13] or precomputed search trees [14]
 90 can simply playback the animation sequence. These approaches
 91 try to reach the goal by connecting series of motion[15], which
 92 sometimes limits the movements of the agents. The main issues
 93 with motion graphs are that they require a very large amount
 94 of animation clips (over 400) and have a high computational
 95 cost which makes them not suitable for large groups of agents
 96 in real-time. Precomputed search trees can handle groups, but

97 work with a few animation clips and are unable to synthesize
 98 new animations.

99 Approaches that ignore animation constraints produce center
 100 of mass trajectories for the animation system to follow. Dif-
 101 ferent models include social forces [2], rule-based approaches [1],
 102 flow tiles [16], roadmaps [17], continuum dynamics [3], and
 103 force models parametrized by psychological and geometrical
 104 rules [4]. These techniques can easily simulate hundreds and
 105 thousands of characters in real-time, but do not account for
 106 locomotion constraints, thus producing artifacts such as foot-
 107 sliding which require correction and simulation updates [5].

108 Considering the root velocity as the input parameter for
 109 character control, numerous approaches can synthesize smooth,
 110 versatile and more plausible locomotion animations [18, 9]. Some
 111 approaches have also used the idea of selecting animations from
 112 a Delaunay triangulation of all the available animation clips
 113 [19, 20]. But all of these approaches are restricted to the root
 114 for performing character control.

115 There has been a recent surge in approaches that produce
 116 footstep trajectories for character control. They can be phys-
 117 ically based but generated off-line [21], be generated online
 118 from an input path computed by a path planner [6], or use sim-
 119 plified control dynamics to produce bio-mechanically plausi-
 120 ble footstep trajectories for crowds [7]. These approaches of-
 121 ten show their animation results off-line using tools such as 3D
 122 Max [22].

123 Footstep-driven animation systems [23] produce unnatural
 124 results using procedural methods. The work in [24] uses a sta-
 125 tistical dynamic model learned from motion capture data in ad-
 126 dition to user-defined space-time constraints (such as footsteps)
 127 to solve a trajectory optimization problem. In [25] random
 128 samples of footsteps make a roadmap going from one point
 129 to another which is used to find a minimum-cost sequence of
 130 motions matching it and then retarget to the exact foot place-
 131 ments. The work in [26, 27] performs a global optimization
 132 over an extracted center of mass trajectory to maximize the
 133 physical plausibility and perceived comfort of the motion, in
 134 order to satisfy the footprint constraints. Recent solutions [6,
 135 28, 29] adopt a greedy nearest-neighbor approach over larger
 136 motion databases. To ensure spatial constraints, the character
 137 is properly aligned with the footsteps and reinforced with in-
 138 verse kinematics, while temporal constraints are satisfied us-
 139 ing time warping. These techniques achieve highly accurate re-
 140 sults in terms of foot positioning, but their computational cost

141 makes them unsuitable for real-time animation of large groups
142 of agents.

143 **Comparison to Prior Work.** Our method produces visually
144 appealing results with foot placement constraints, using only a
145 handful of motion clips, and can seamlessly follow footstep-
146 based control trajectories while preserving the global appear-
147 ance of the motion. Compared to [9], we exploit the combi-
148 nation of multiple parameter spaces for footstep-precision con-
149 trol. This reduces the dimensionality of the problem, compared
150 to [29]. Unlike previous work in the literature, our method can
151 synthesize animations for a large number of characters in real
152 time, following footstep trajectories for different walking styles
153 and even running motions with a small flying phase.

154 3. Framework Overview

155 Animating characters in real time animations has different
156 requirements depending on the application. In many applica-
157 tions, the user only wants to control the direction of movement
158 and speed of the root, but there are other situations where a
159 finer control of the foot positioning is required. For example,
160 the user may want to respect different walking gaits depending
161 on the terrain, to make the character step over stones to cross
162 a river, or walk through some space full of holes whilst avoid-
163 ing falling. For this purpose we have developed a framework to
164 animate virtual characters following footstep trajectories, while
165 still being able to follow trajectories based on the movement of
166 the COM when necessary.

167 Online locomotion systems [9] traditionally produce syn-
168 thesized motions that follow a COM trajectory, with procedural
169 corrections for uneven terrain. These methods can nicely fol-
170 low COM trajectories, but they lack control over the style of
171 walking and the kind of steps. For instance, we cannot control
172 whether in order to walk fast, the character will move with large
173 distances between steps or with a fast sequence of short steps.
174 This is the main issue we address in our work: to provide an
175 animation system that is able to accurately follow footstep tra-
176 jectories while meeting real-time constraints, and that can scale
177 to handle large groups of animated characters .

178 For this purpose, we introduce two parametric spaces based
179 on the position of each foot: Ω_{f_L} and Ω_{f_R} , and switch between
180 the two depending on the swing foot, as well as a parametric
181 space based on the root movement Ω_{f_R} . Our technique takes
182 into account both displacement (from Ω_{f_L} and Ω_{f_R}) and speed
183 (from Ω_r) to ensure the satisfaction of both spatial and temporal
184 constraints. Our system provides the user with the flexibility
185 to choose between different control granularities ranging from
186 exact foot positioning to exact root velocity trajectories. Fig. 2
187 shows our framework.

188 4. Footstep-based Locomotion

189 The main goal of the Footstep-based Locomotion Controller
190 is to accurately follow a footstep trajectory, i.e., to animate a
191 fully articulated virtual human to step over a series of foot-
192 plants with space and velocity constraints. The system must

193 meet real-time constraints for a group of characters, should be
194 robust enough to handle sparse motion clips, and needs to pro-
195 duce synthesized results that are void of artifacts such as foot
196 sliding and collisions.

197 4.1. Motion Clip Analysis

198 From a collection of cyclic motion clips¹, we need to extract
199 individual footsteps. Each motion clip contains two steps, one
200 starting with the left foot on the floor, and one starting with
201 the right foot. A step is defined as the action where one foot
202 of the character starts to lift-off the ground, moves in the air
203 and finishes when it is again planted on the floor. We say that
204 a footstep corresponds to one foot when that foot is the one
205 performing the action previously described. The foot that stays
206 in contact with the floor for most of the duration of the footstep
207 is called the supporting foot, since it supports the weight of the
208 body. This applies even for running motions, where the support
209 foot goes into fly mode for a short phase of the footstep, but it is
210 still the one supporting the weight during most of the footstep.

211 During an offline analysis, each motion clip m_i is annotated
212 with the following information: (1) \mathbf{v}_i^r : Root velocity vector. (2)
213 \mathbf{d}_i^L : Displacement vector of the left foot. (3) \mathbf{d}_i^R : Displacement
214 vector of the right foot.

215 Similar to [9], animations are analyzed in place, that is, we
216 ignore the original root forward displacement, but keep the ver-
217 tical and lateral deviations of the motion. This allows an auto-
218 matic detection of foot events, such as lifting, landing or plant-
219 ing, from which we can deduce the displacement vector of each
220 foot. For example, the displacement vector of the left foot \mathbf{d}_i^L
221 is obtained by subtracting the right foot position at the instant
222 of time when the left foot lands, from the right foot position
223 at the instant of time when the left foot is lifting off. These
224 displacements will be later used to move the whole character,
225 eliminating any foot sliding. By adding \mathbf{d}_i^L to \mathbf{d}_i^R and knowing
226 the time duration of the clip, we can calculate the average root
227 velocity vector \mathbf{v}_i^r of the clip m_i .

228 This average velocity is used to classify and identify ani-
229 mations, by providing an example point which is the input
230 for the polar gradient band interpolator (where each example
231 point represents a velocity in a 2D parametric space). Gradi-
232 ent band interpolation specifies an influence function associ-
233 ated with each example, which creates gradient bands between
234 the example point and each of the other example points. These
235 influence functions are normalized to get the weight functions
236 associated with each example. However the standard gradient
237 band interpolation is not well suited for interpolation of exam-
238 ples based on velocities. The polar gradient band interpolation
239 method is based on reasoning that in order to get more desir-
240 able behavior for the weight functions of example points that
241 represent velocities, the space in which the interpolation takes
242 place should take on some of the properties of a polar coordi-
243 nate system. It allows for dealing with differences in direction

¹Although cyclic animations are not strictly required by our method, they help find smoother transitions between consecutive footsteps and are preferred by most standard animation systems [9].

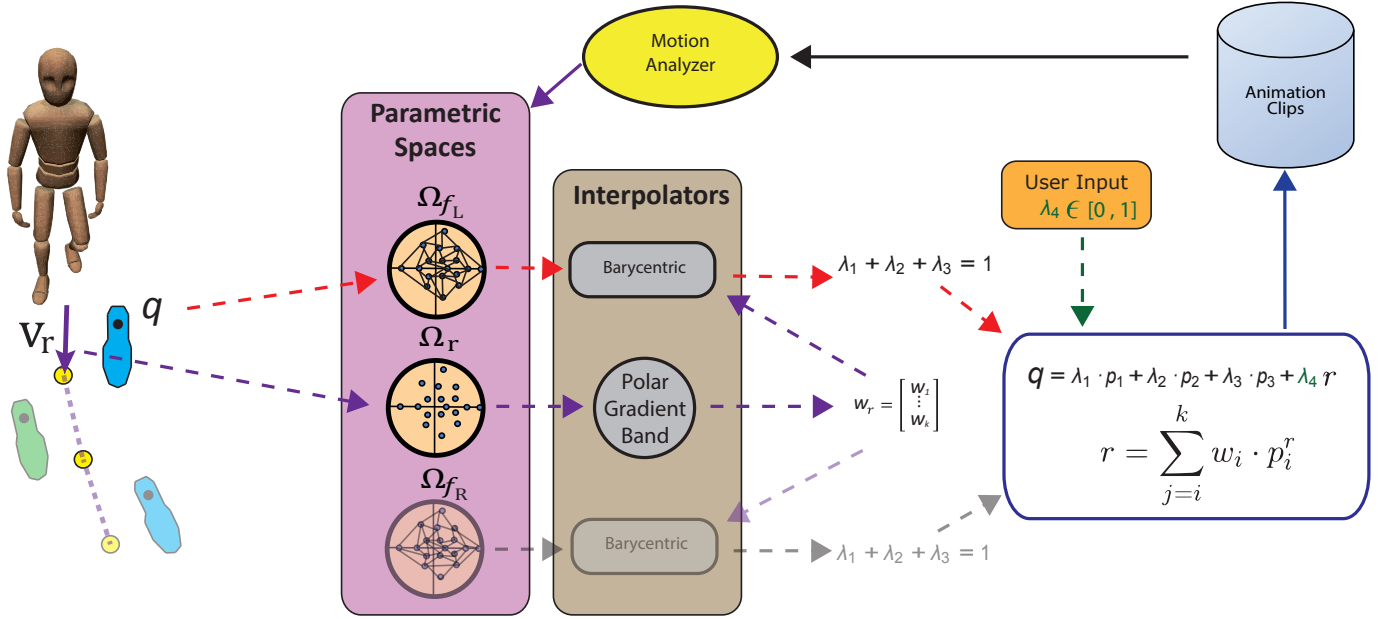


Figure 2: Online selection of the blend weights to accurately follow a footstep trajectory. Ω_r uses a gradient band polar based interpolator [9] to give a set of weights w_j , which are then used by the barycentric coordinates interpolator to tradeoff between footstep and COM accuracy.

244 and magnitude rather than differences in the Cartesian vector
 245 coordinate components. For more details we refer the reader to
 246 [9].

247 Each motion clip is then split into two animation steps A_i^L
 248 for the left foot and A_i^R for the right foot. For each foot, we need
 249 to calculate all the possible positions that can be reached based
 250 on the set of animation steps available. Since the same analysis
 251 is performed for both feet separately, from now on we will not
 252 differentiate between left and right for the ease of exposition.
 253 For each individual step animation A_i and given an initial root
 254 position, we want to extract the foot landing position p_i , if the
 255 corresponding section of its original clip was played. This is
 256 calculated by summing the root displacement during the section
 257 of the animation with the distance vector between the root
 258 projection over the floor and the foot position in the last frame.

259 The set $\{p_i | \forall i \in [1, n]\}$ where n is the number of step ani-
 260 mations, provides a point cloud. Fig. 3 shows the Delaunay
 261 triangulation that is calculated for the point cloud of landing
 262 positions. This triangulation is queried in real time to deter-
 263 mine the simplex that contains the next footstep in the input
 264 trajectory. Once the triangle is selected, we will use its three
 265 vertices p_1 , p_2 and p_3 to compute the blending weights for each
 266 of the corresponding animations A_1 , A_2 and A_3 .

267 4.2. Footstep and Root Trajectories

268 Our system can work with both footstep trajectories and
 269 COM trajectories. A footstep trajectory will be given as an ordered
 270 list of space-time positions with orientations, whether it
 271 is precomputed or generated on-the-fly.

272 The input footstep trajectory may be accompanied by its as-
 273 sociated root trajectory (a space-time curve, rather than a list of
 274 points, and an orientation curve), or else we can automatically
 275 compute it from the input footsteps by interpolation. This is

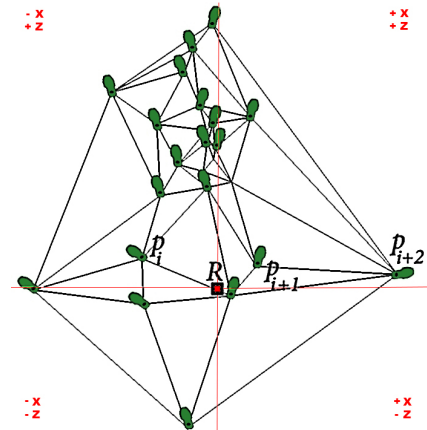


Figure 3: Delaunay triangulation for the vertices representing the landing positions ($p_i, p_{i+1}, p_{i+2}, \dots$) of the left foot when the root, R , is kept in place.

276 achieved by computing the projection of the root on the ground
 277 plane, as the midpoint of the line segment joining two consecu-
 278 tive footsteps. The root orientation is then computed as the
 279 average between the orientation vectors of each set of consecu-
 280 tive steps. This provides us with a sequence of root positions
 281 and orientations which can be interpolated to approximate the
 282 motion of the root over the course of the footstep trajectory.

283 4.3. Online Selection

284 During run time, the system animates the character towards
 285 the current target footstep. If the target is reached, the next foot-
 286 step along the trajectory is chosen as the next target. For each
 287 footstep q_j in the input trajectory $\{q_1, q_2, q_3, \dots, q_m\}$ we need to
 288 align the Delaunay triangulation graph with the current root posi-
 289 tion and orientation. Then the triangle containing the next foot

290 position is selected as the best match to calculate the weights re-
 291 quired to nicely blend between the three animations in order to
 292 achieve a footstep that will land as close as possible to the de-
 293 sired destination position q_j (Fig. 4). Notice that these weights
 294 are applied equally to all the joints in the skeleton, which means
 295 that at this stage we cannot accurately adjust the specific foot
 296 orientation required by each footstep in the input trajectory.

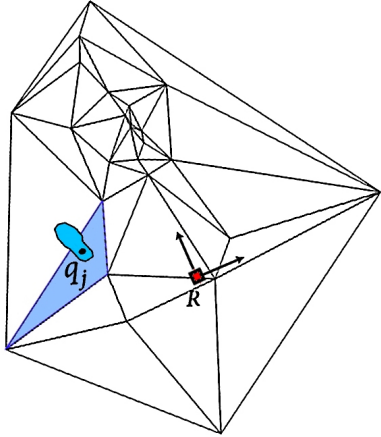


Figure 4: By matching root position and orientation, we can determine the triangle containing the destination position for the landing position q_j .

297 4.4. Interpolation

298 Footstep parameters change between successive footplants,
 299 remaining constant during the course of a single footstep (sev-
 300 eral frames of motion). Therefore we need to compute the best
 301 interpolation for each footstep, blend smoothly between con-
 302 secutive steps, and apply the right transformation to the root in
 303 order to avoid foot-sliding or intersections with the ground.

304 To meet these requirements, we use a barycentric coordi-
 305 nates based interpolator in Ω_{f_L} and Ω_{f_R} , and constrain the so-
 306 lution based on the weights computed in Ω_r . This allows us to
 307 animate a character at the granularity of footsteps, while simul-
 308 taneously accounting for the global motion of the full body.

309 If we only consider the footstep parametric space, then the
 310 vertices of the selected triangle are those that can provide the
 311 best match for the desired foot position. The barycentric co-
 312 ordinates of the desired footstep are calculated for the selected
 313 triangle as the coordinates that satisfy:

$$q_j = \lambda_1 \cdot p_1 + \lambda_2 \cdot p_2 + \lambda_3 \cdot p_3, \quad (1)$$

$$\lambda_1 + \lambda_2 + \lambda_3 = 1$$

314 where p_1 , p_2 and p_3 are the positions of the foot landing if we
 315 run animation steps A_1 , A_2 and A_3 respectively. The calculated
 316 barycentric coordinates are then used as weights for the blend-
 317 ing between animations. A nice property of the barycentric co-
 318 ordinates is that the sum equals 1, which is a requirement for
 319 our blending. Finally in order to move the character towards
 320 the next position, we need to displace the root of the character
 321 adequately to avoid foot sliding. The final root displacement

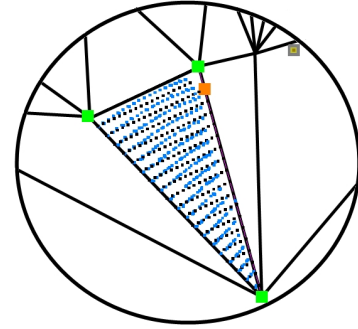


Figure 5: Offsets for different landing positions in a triangle, between barycentric coordinates interpolation (black dots) and blending the whole skeleton using SLERP (blue dots).

322 vector, \mathbf{d}'_j is calculated as the weighed sum of the root's dis-
 323 placement of the three selected animation steps (Eq. 2), and
 324 changes in orientation of the input root trajectory are applied as
 325 rotations over the ball of the supporting foot.

$$\mathbf{d}'_j = \lambda_1 \cdot \mathbf{d}'_1 + \lambda_2 \cdot \mathbf{d}'_2 + \lambda_3 \cdot \mathbf{d}'_3 \quad (2)$$

326 This provides a final root displacement that is the result of
 327 interpolating between the three root displacements in order to
 328 avoid any foot sliding. It is important to notice that the barycen-
 329 tric coordinates provide the linear interpolation required be-
 330 tween three points in 2D space to obtain the position q_j . This
 331 is an approximation of the real landing position that our char-
 332 acter will reach, as the result of blending the different poses of
 333 the three animation clips, using spherical linear interpolation
 334 (SLERP) with a simple iterative approach as described in [30].

335 Therefore there will be an offset between the desired posi-
 336 tion q_j and the position reached after interpolating the three an-
 337 imations. To illustrate this offset, Fig. 5 shows the points sam-
 338 pled to compute barycentric coordinates in black, and in blue
 339 the real landing positions achieved after applying the barycen-
 340 tric weights to the animation engine and performing blending
 341 using SLERP. In order to correct this small offset at the same
 342 time that we adjust the feet to the elevation of the terrain and
 343 orient the footstep correctly, we incorporate a fast and simple
 344 IK solver.

345 4.5. Inverse Kinematics

346 An analytical IK solver modifies the leg joints in order to
 347 reach the desired position at the right time with a pose as close
 348 as possible to the original motion capture data. For footstep-
 349 based control, the desired foot position is already encoded in the
 350 footstep trajectory, and for COM trajectories the final position is
 351 calculated by projecting the current position of the foot over the
 352 terrain. The controller feeds the IK system with the end position
 353 and orientation for each footstep. This allows the system to
 354 handle footsteps on uneven terrain.

355 5. Incorporating Root Movement Fidelity

356 In some scenarios the user may be more interested in fol-
 357 lowing root velocities than in placing the feet at exact footsteps

358 or with specific walking styles. We present a solution to include
 359 root movement based interpolation in our current barycentric
 360 coordinates based interpolator through a user controlled param-
 361 eter λ_4 .

362 For this purpose, we incorporate the locomotion system pre-
 363 sented by Johansen [9] to produce synthesized motions that
 364 follow a COM trajectory with correction for uneven terrain.
 365 During offline analysis, a parametric space is defined using all
 366 the root velocity vectors extracted from the clips in the motion
 367 database. For example, a walk forward clip at 1.5 m/s, and a
 368 left step clip at 0.5 m/s produces a parametric space using the
 369 root velocity vectors going from the forward direction to the
 370 90° direction, and with speeds from 0.5 m/s to 1.5 m/s.

371 Given a desired root velocity we define a parametric space
 372 Ω_r , and a gradient band interpolator in polar space [9] is created
 373 to compute the weights for each animation clip to produce the
 374 final blended result. The gradient band interpolator does not en-
 375 sure accuracy of the produced parameter values but it does en-
 376 sure smooth interpolation under dynamically and continuously
 377 changing parameter values, as with a player-controlled char-
 378 acter. Once the different clips are blended with the computed
 379 weights, the system predicts the support foot position at the end
 380 of the cycle and projects it on the ground to find the exact posi-
 381 tion where it should land.

382 The root movement based interpolator will select a set of k
 383 animations A_1^r to A_k^r with their corresponding weights: w_1, \dots, w_k .
 384 Each of those animations provides a landing position p_1^r, \dots, p_k^r ,
 385 and if we only interpolated these animations we would obtain
 386 the landing point r .

387 In order to incorporate the output of the polar gradient band
 388 interpolator in the barycentric coordinates based interpolator
 389 we proceed as indicated in Algorithm 1.

390 The algorithm first checks whether a vertex of the current
 391 triangle $\langle p_1, p_2, p_3 \rangle$ can be replaced by any of the three vertices
 392 with highest weights selected by the polar band interpolator, p_j^r ,
 393 $j \in [1, k]$ (lines 1-13 in the algorithm). This replacement takes
 394 place if the distance between the two landing positions p_i and
 395 p_j^r is within a user input threshold ϵ (line 7), and the resulting
 396 triangle still contains the desired landing position q_j (function
 397 *IsInTriangle* returns true if q_j is inside the new triangle). This
 398 means that there is another animation that also provides a valid
 399 triangle and has a root velocity that is closer to the input root
 400 velocity.

401 Next, function *CalculateRootLanding* computes the landing
 402 position reached after blending the animations given by the root
 403 movement interpolator (Eq. 3).

$$r = \sum_{i=1}^k w_i \cdot p_i^r \quad (3)$$

404 Finally, *ComputeWeights* calculates the three λ_i for the next
 405 footstep q_j by incorporating a user provided λ_4 and the result of
 406 the polar band interpolator r (Eq. 4).

$$q_j = \lambda_1 \cdot p_1 + \lambda_2 \cdot p_2 + \lambda_3 \cdot p_3 + \lambda_4 \cdot r \quad (4)$$

Algorithm 1 Incorporating root movement fidelity

Input:

- The target position q_j ,
- The current triangle $\langle p_1, p_2, p_3 \rangle$,
- Root landing positions $\langle p_1^r, \dots, p_k^r \rangle$,
- Animation weights $\langle w_1, \dots, w_k \rangle | w_1 \geq \dots \geq w_k$,
- A user input threshold ϵ ,
- A user input weight parameter λ_4

Output: $\lambda_1, \lambda_2, \lambda_3$

```

1: for  $i = 1$  to 3 do
2:    $u \leftarrow (i + 1) \bmod 3$ 
3:    $v \leftarrow (i + 2) \bmod 3$ 
4:    $j \leftarrow 1$ 
5:    $replaced \leftarrow \text{false}$ 
6:   while  $j \leq 3 \wedge \neg replaced$  do
7:     if  $\|p_i - p_j^r\| \leq \epsilon \wedge \text{IsInTriangle}(q_j, \langle p_j^r, p_u, p_v \rangle)$ 
8:       then
9:          $p_i \leftarrow p_j^r$ 
10:         $replaced \leftarrow \text{true}$ 
11:     end if
12:      $j \leftarrow j + 1$ 
13:   end while
14: end for
15:  $r \leftarrow \text{CalculateRootLanding}(\langle p_1^r, \dots, p_k^r \rangle, \langle w_1, \dots, w_k \rangle)$ 
16:  $\langle \lambda_1, \lambda_2, \lambda_3 \rangle \leftarrow \text{ComputeWeights}(\langle p_1, p_2, p_3 \rangle, \lambda_4, r)$ 

```

and λ_i are defined using the following relationship:

$$\lambda_1 + \lambda_2 + \lambda_3 + \lambda_4 = 1 \quad (5)$$

407 Since w_i and p_i^r are known $\forall i \in \{1, \dots, k\}$, and λ_4 is a user in-
 408 put, we have a linear system, where λ_4 determines the trade-off
 409 between following footsteps accurately (if $\lambda_4 = 0$), and simply
 410 following root movement (if $\lambda_4 = 1$).

411 As the user increases λ_4 there will be a value $\beta \in [0, 1]$ for
 412 which λ_1, λ_2 or λ_3 will be negative, when solving the system
 413 of equations formed by eq.4 and eq.5. In order to avoid anima-
 414 tion artifacts it is necessary to deal only with positive weights,
 415 therefore we guarantee that the system will only reproduce q_j
 416 accurately as long as $\lambda_4 < \beta$. If we further increase λ_4 beyond
 417 the value β then the algorithm will provide the blending values
 418 that correspond to a new point q' which is the result of a linear
 419 interpolation between q_j and point r . When $\lambda_4 = 1$ the result-
 420 ing blending will be exclusively the one provided by the root
 421 movement trajectory since $\lambda_1 = \lambda_2 = \lambda_3 = 0$. Fig. 6 illustrates
 422 this situation.

423 **Time Warping.** Incorporating root velocity in the interpola-
 424 tion, does not always guarantee that the time constraints as-
 425 signed per footstep will be satisfied. Therefore once we have
 426 the final set of animations to interpolate between, with their
 427 corresponding weights $\lambda_i, i \in \{1, 2, 3\}$ and $w_j, j \in [1, k]$, we
 428 need to apply time warping. Each input footstep f_m has a time
 429 stamp τ_m indicating the time at which position q_m should be
 430 reached (where $m \in [1, M]$ and M is the number of footsteps in
 431 the input trajectory). The total time of the current motion, T can

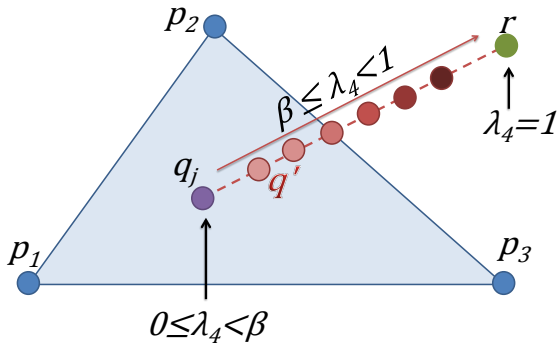


Figure 6: When solving the system of equations given by eq.4 and eq.5, the value of either λ_1 , λ_2 or λ_3 will be negative when $\lambda_4 \geq \beta$. Therefore we need to calculate the barycentric coordinates for a new point q' which moves linearly from q_j to r as the user increases the value of λ_4 from β to 1. This means solving the system of equations for q' instead of q_j , as it is the closest point to the desired landing position which guarantees that all weights in eq. 5 will be positive.

432 be calculated as the weighted sum of the time of the animation
 433 steps being interpolated: $T = \sum_{i=1}^3 (\lambda_i \cdot t(A_i)) + \sum_{j=1}^k (w_j \cdot t(A_j))$.
 434 Therefore the time warping factor that needs to be applied can
 435 be calculated as: $warp_m = (\tau_m - \tau_{m-1})/T$.

436 **Outside the Convex-Hull.** The footstep parametric space defines a convex-hull delimiting the area where our character can land its feet. When our target footstep position falls inside this area, clips can be interpolated to reach that desired position. But if it falls outside this convex-hull we still want the system to consider and try to reach it. Our solution to handle this problem consists of projecting orthogonally the input landing position q over the convex-hull to a new position q_{proj} . Our system then gives the blending weights for q_{proj} and applies IK to adjust the final position. We include a parameter to define a maximum distance for the IK to set an upper limit on the correction of the landing position. It is important to notice that even if the input trajectory has some footsteps that are unreachable with the current data base of animation clips, our system will provide a synthesized animation that will follow the input trajectory as closely as possible, until it recovers and catches up with future steps in the input trajectory. This situation is similar to the scenarios where the user increases λ_4 and then reduces it again.

454 6. Results

455 The animation system described in the paper is implemented
 456 in C# using the Unity 3D Engine [31]. The footstep trajectories
 457 used to animate the characters are generated using the method
 458 described in [7] or are created by the user. Some difficult scenarios, exercising careful footstep selection, are shown in Fig. 1 and Fig. 7. Agents carefully plant their feet over pillars (Fig. 7-a) or use stepping stones to avoid falling into the water (Fig. 7-b). We show our ability to handle over a hundred agents at 13 FPS (Fig. 7-c and Fig. 9). The supplementary video demon-

464 strates additional results (high resolution video², low resolution
 465 video³).

466 **Obstacle Course.** We exercise the locomotion dexterity of a
 467 single animated character in an obstacle course. The character
 468 follows a footstep trajectory with different walking gaits , alter-
 469 nating running and walking phases (Fig. 1-a,b), and including
 470 sidesteps (Fig. 1-c) and backward motion (Fig. 1-e).

471 **Stepping Stone Problem.** Stepping stone problems (Fig. 7-
 472 b) require careful footstep level precision where constraints re-
 473 quire the character to place their feet exactly on top of the stones
 474 in order to successfully navigate the environment. Our frame-
 475 work can be coupled with footstep-based controllers to solve
 476 these challenging benchmarks.

477 **Integration with Crowd Simulator.** We integrate our ani-
 478 mation system with footstep-based simulators [7]; our charac-
 479 ter follows the simulated trajectories without compromising its
 480 motion fidelity while scaling to handle large crowds of charac-
 481 ters (Fig. 7-c).

482 It is important to mention that the quality of the results de-
 483 pends strongly on the quality of the clips available from the
 484 motion capture library. As can be seen in the video, the least
 485 precise movements in our results are side steps and back steps.
 486 This is due to two reasons: (1) we had a small number of ani-
 487 mations compared to other walking gaits, and thus triangles
 488 covering that space have larger areas, and (2) interpolation ar-
 489 tifacts appear when blending between animations that move in
 490 opposite directions (for example a backwards step with a for-
 491 ward step). We believe that having a better and denser sam-
 492 pling in these areas will improve the results. For steps falling in
 493 triangles of smaller areas, and with all the vertices in the same
 494 quartile we have obtained results of high quality even for diffi-
 495 cult animations such as running or performing small jumps.

496 6.1. Foot Placement Accuracy

497 The presented barycentric coordinates interpolator assumes
 498 a small offset between the results of linearly interpolating lan-
 499 ding positions from the set of animations being blended, and the
 500 actual landing position when calculating spherical linear inter-
 501 polation over the set of quaternions. This small offset depends
 502 on the area of the triangle, so as we incorporate more anima-
 503 tions into our data base, we obtain a denser sampling of landing
 504 positions and thus reduce both the area of the triangles and the
 505 offset. We believe this is a convenient trade off since such a
 506 small offset can be eliminated with a simple analytical solver
 507 but the efficiency of computing barycentric coordinates offers
 508 great performance. It is also important to notice that if exact
 509 foot location is not necessary, and the user only needs to indi-
 510 cate small areas for stepping as in the water scenario, then it is
 511 not necessary to apply the IK correction. Fig. 8 shows the offset
 512 between the landing position and the footstep. The magnitude
 513 of the error is illustrated as the height of the red cylinders that
 514 are located at the exact location where the foot first strikes.

²<https://www.dropbox.com/s/o1b9w73qd45fmip/videoCAG.mp4?dl=0>

³<https://www.dropbox.com/s/ptdz788f2k9ad3g/videoCAGlowRes.mp4?dl=0>

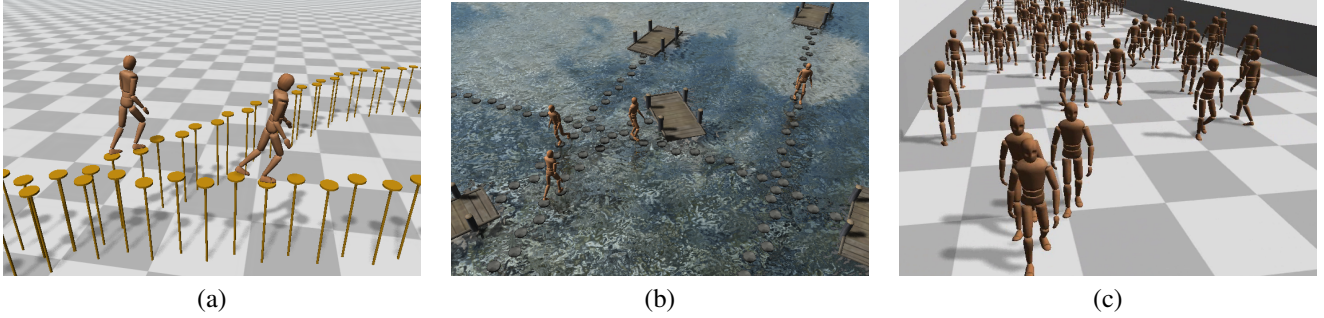


Figure 7: (a) Agents accurately following a footstep trajectory and avoiding falls by carefully stepping over pillars. (b) The stepping stone problem is solved with characters avoiding falls into the water. (c) A crowd of over 100 agents simulated at interactive rates.

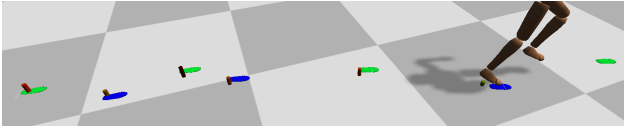


Figure 8: The red columns show the small offset between landing position and the footstep when the IK corrections are not being applied.

7. Conclusions and Future Work

We have presented a system that uses multiple parameter spaces to animate fully embodied virtual humans to accurately follow a footstep trajectory respecting root velocities, using a relatively small number of animation clips (24 in our examples). Our method is fast enough to be used with tens of characters in real time (25 FPS) and over a hundred characters at 13 FPS. The method can handle uneven terrain, and can be easily extended to introduce additional locomotion behaviors by grouping new sets of animation clips and generating different parametric spaces. For example, walking and running motions can be blended together, but if we wanted to add crawling motions or jumping motions, it would be better to separate them in different parametric spaces for each style. This will avoid unnatural interpolations that can appear when blending between very different styles. Having different parametric spaces requires some sort of classification, which could initially be done manually but it could also be based on the characteristics of the motion, such as changes in acceleration, maximum heights of the root, length of fly phase, etc. Assuming we can extract the parametric spaces for different animation types, it would also be necessary in some cases to have additional transition clips to switch between very different locomotion types, i.e. crawling and walking.

We do not run physical or biomechanical simulations, and use interpolation and blending between motion capture animations. Our method accuracy depends on the variety of animation clips, while its quality and efficiency depends on the number of clips. A trade-off between efficiency and accuracy is therefore necessary, for which we have found a good equilibrium.

Limitations. In order to reduce the dimensionality of the problem, we have not included in our parametric space the orientation of the previous footstep. Ignoring the final orientation of the character at the end of the previous step can induce some discontinuities between footsteps. We mitigate this effect by blending between footsteps automatically for a small amount of time (about 0.2 seconds) at the advantage of reducing the computational time and thus making our method suitable for large groups of agents in real time. Regarding the selection of animation at the end of each footstep, notice that in our database, left and right animation steps are extracted from complete animation cycles that are usually consistent in parameters such as

6.2. Performance

Fig. 9 shows the frame rate we obtain as we double the number of agents. It is important to notice that increasing the number of animations would enhance the quality and accuracy of the results, with just a small overhead on the performance.

The average time of the locomotion controller is 0.43ms, this process includes blending animations, IK, the polar band interpolator and our barycentric coordinates based interpolator. The computational cost of our footstep interpolator is 0.2 ms, which is amortized over several frames as the interpolation in Ω_{f_L} or Ω_{f_R} only need to be performed once per footstep. This time is divided between computing the root movement polar band interpolator which takes 0.155ms and our barycentric coordinates interpolator which takes 0.045ms. Performance results were measured on an Intel Core i7-2600k CPU at 3.40GHz with 16GB RAM.

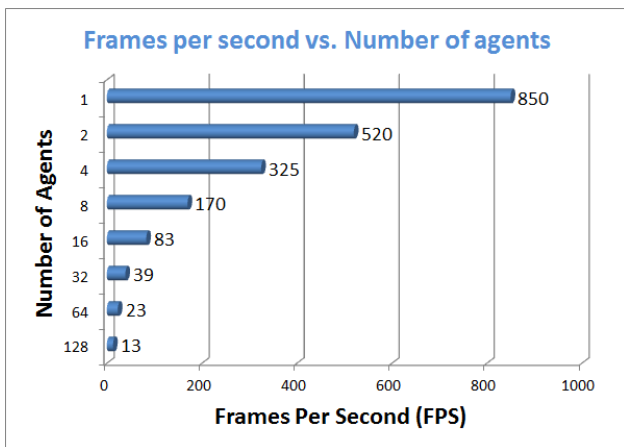


Figure 9: Performance of the Footstep Locomotion System in frames per second as the number of agents increases.

573 velocity, acceleration and walking gait. Therefore for a given
 574 sequence of steps, the most likely animation steps to be chosen
 575 will be those extracted from the same set of animation cycles,
 576 thus resulting in smooth and natural transitions between very
 577 similar steps. When the characteristics of the steps change drastically,
 578 then our method needs to blend between steps from very
 579 different animation cycles. So in general, alternating left/right
 580 steps results in natural transitions with smooth continuity when
 581 blending animations, and only when the input step trajectory
 582 changes drastically between each pair of steps, we may observe
 583 transitions between animations that feel unnatural. This can
 584 happen if the step trajectory is done manually with artifacts due
 585 to the user's lack of experience creating footstep trajectories,
 586 or for example when the input trajectory forces the character to
 587 walk over artificially located steps, like crossing a river by stepping
 588 over stones. We would like to emphasize that this situation
 589 would also look awkward in the real world and thus the result
 590 of our synthesized animation may be the desired one.

591 **Future Work.** For future work we would like to extend our
 592 barycentric coordinates interpolator to 3D space with the third
 593 coordinate being the root velocity. This will free our system
 594 from the polar band interpolator which not only takes longer to
 595 compute but also selects too many animations which results in
 596 slower blending. One thing to explore could be to interleave the
 597 execution of the Footstep-based Locomotion Controller from
 598 different characters in different frames, ensuring we do not execute
 599 it for all the agents in the crowd.

600 Acknowledgements

601 This work has been partially funded by the Spanish Ministry
 602 of Science and Innovation under Grant TIN2010-20590-C02-
 603 01. A. Beacco is also supported by the grant FPUAP2009-2195
 604 (Spanish Ministry of Education). The research reported in this
 605 document/presentation was also performed in connection with
 606 Contract Number W911NF-10-2-0016 with the U.S. Army Research
 607 Laboratory. The views and conclusions contained in this
 608 document are those of the authors and should not be interpreted
 609 as presenting the official policies or position, either expressed
 610 or implied, of the U.S. Army Research Laboratory, or the U.S.
 611 Government. Citation of manufacturers or trade names does not
 612 constitute an official endorsement or approval of the use thereof.
 613 The U.S. Government is authorized to reproduce and distribute
 614 reprints for Government purposes notwithstanding any copy-
 615 right notation hereon.

616 References

617 [1] C. W. Reynolds, Flocks, herds and schools: A distributed behavioral
 618 model, in: ACM SIGGRAPH, Vol. 21, 1987, pp. 25–34.
 619 [2] D. Helbing, I. Farkas, T. Vicsek, Simulating dynamical features of escape
 620 panic, *Nature* 407 (2000) 487–490.
 621 [3] A. Treuille, S. Cooper, Z. Popović, Continuum crowds, in: ACM Transactions
 622 On Graphics, Vol. 25, 2006, pp. 1160–1168.
 623 [4] N. Pelechano, J. M. Allbeck, N. I. Badler, Controlling individual agents
 624 in high-density crowd simulation, in: ACM Symposium on Computer
 625 Animation, 2007, pp. 99–108.

626 [5] N. Pelechano, B. Spanglang, A. Beacco, Avatar Locomotion in Crowd
 627 Simulation, *International Journal of Virtual Reality* 10 (2011) 13–19.
 628 [6] A. Egges, B. van Basten, One Step at a Time: Animating Virtual Characters
 629 Based on Foot Placement, *The Visual Computer* 26 (6-8) (2010)
 630 497–503.
 631 [7] S. Singh, M. Kapadia, G. Reinman, P. Faloutsos, Footstep Navigation
 632 for Dynamic Crowds, *Computer Animation and Virtual Worlds* 22 (2011)
 633 151–158.
 634 [8] A. Treuille, Y. Lee, Z. Popović, Near-Optimal Character Animation with
 635 Continuous Control, *ACM Transactions on Graphics* 26 (3) (2007) 7.
 636 [9] R. S. Johansen, Automated Semi-Procedural Animation, Master Thesis.
 637 URL <http://runevision.com/thesis/>
 638 [10] L. Kovar, M. Gleicher, F. Pighin, Motion graphs, in: ACM SIGGRAPH,
 639 2002, pp. 473–482.
 640 [11] L. Zhao, A. Safonova, Achieving Good Connectivity in Motion Graphs,
 641 *Graphical Models* 71 (4) (2009) 139–152.
 642 [12] C. Ren, L. Zhao, A. Safonova, Human Motion Synthesis with
 643 Optimization-Based Graphs, *Computer Graphics Forum* 29 (2).
 644 [13] J. Min, J. Chai, Motion Graphs++, *ACM Transactions On Graphics* 31 (6)
 645 (2012) 1.
 646 [14] M. Lau, J. J. Kuffner, Precomputed search trees: planning for interactive
 647 goal-driven animation, in: ACM Symposium on Computer Animation,
 648 2006, pp. 299–308.
 649 [15] A. Witkin, Z. Popovic, Motion warping, in: ACM SIGGRAPH, 1995, pp.
 650 105–108.
 651 [16] S. Chenney, Flow tiles, in: ACM Symposium on Computer Animation,
 652 2004, pp. 233–242.
 653 [17] A. Sud, E. Andersen, S. Curtis, M. Lin, D. Manocha, Real-time path plan-
 654 ning for virtual agents in dynamic environments, in: *IEEE Virtual Reality*,
 655 2007, pp. 91–98.
 656 [18] P. Gardon, R. Boulic, D. Thalmann, Robust on-line adaptive footplant
 657 detection and enforcement for locomotion, *The Visual Computer* 22 (3)
 658 (2006) 194–209.
 659 [19] J. Pettré, J.-P. Laumond, T. Siméon, A 2-stages locomotion plan-
 660 ner for digital actors, in: *Proceedings of the 2003 ACM SIG-*
 661 *GRAPH/Eurographics Symposium on Computer Animation, SCA '03,*
 662 *Eurographics Association, Aire-la-Ville, Switzerland, Switzerland, 2003,*
 663 *pp. 258–264.*
 664 [20] J. Pettré, J.-P. Laumond, A motion capture-based control-space approach
 665 for walking mannequins: Research articles, *Computer Animation and*
 666 *Virtual Worlds* 17 (2) (2006) 109–126.
 667 [21] M. Felis, K. Mombaur, Using Optimal Control Methods to Generate Human
 668 Walking Motions, *Motion in Games* (2012) 197–207.
 669 [22] Autodesk, 3d studio max,
 670 www.autodesk.com/products/autodesk-3ds-max/overview (2014).
 671 [23] M. Girard, A. A. Maciejewski, Computational modeling for the computer
 672 animation of legged figures, in: *SIGGRAPH, ACM, 1985,* pp. 263–270.
 673 [24] J. Chai, J. K. Hodgins, Constraint-Based Motion Optimization Using A
 674 Statistical Dynamic Model, *ACM SIGGRAPH*.
 675 [25] M. G. Choi, J. Lee, S. Y. Shin, Planning biped locomotion using motion
 676 capture data and probabilistic roadmaps, *ACM Transactions on Graphics*
 677 22 (2) (2003) 182–203.
 678 [26] H. Ko, N. I. Badler, Animating human locomotion with inverse dynamics,
 679 *IEEE Computer Graphics & Applications* 16 (2) (1996) 50–59.
 680 [27] M. van de Panne, From Footprints to Animation, *Computer Graphics Forum*
 681 16 (4) (1997) 211–223.
 682 [28] B. van Basten, P. W. A. M. Peeters, A. Egges, The Step Space : Example-
 683 Based Footprint-Driven Motion Synthesis, *Computer Animation and Virtual*
 684 *Worlds* 21 (May) (2010) 433–441.
 685 [29] B. van Basten, S. Stüvel, A. Egges, A Hybrid Interpolation Scheme for
 686 Footprint-Driven Walking Synthesis, *Graphics Interface* (2011) 9–16.
 687 [30] A. Shoulson, N. Marshak, M. Kapadia, N. I. Badler, ADAPT : The Agent
 688 Development and Prototyping Testbed, *ACM SIGGRAPH I3D*.
 689 [31] Unity, Unity - game engine (2014).
 690 URL <http://unity3d.com/>